JOURNAL OF MATERIALS SCIENCE 32 (1997) 3411–3417

Application of electron beam lithography to study microcreep deformation and grain boundary sliding

S. KISHIMOTO, N. SHINYA
National Research Institute for Metals, 1-2-1, Sengen, Tsukuba, Ibaraki 305, Japan
M. D. MATHEW
Indira Gandhi Centre for Atomic Research, Kalpakkam 603102, India

Electron beam lithography has been employed to study microcreep deformation and grain boundary sliding in pure copper. Fine electron-sensitive microgrids of an alloy of palladium and gold were developed on the surface of rectangular specimens. Interrupted creep tests were carried out at 723 K at two stress levels in an argon atmosphere. Creep strain and grain boundary sliding were determined by forming Moiré fringes in a scanning electron microscope as well as from the displacement of the grid lines. Local distribution of creep strain inside the grains was found to be non-uniform. Grain boundary sliding exhibited a wavy behaviour.

1. Introduction

Under creep conditions, polycrystalline materials undergo various deformation and damage processes such as slip, grain boundary sliding, grain boundary migration, as well as nucleation and growth of cavities on grain boundaries. These matrix and grain boundary processes are closely interrelated; for example, matrix deformation influences grain boundary sliding and vice versa. The intergranular processes are also governed by the grain boundary features of the material such as grain boundary structure, misorientation of the grain boundary, viscosity of the grain boundary, type of grain boundary, namely, random versus coincidence site lattice, etc. [1–4]. Due to the heterogeneity in these grain boundary features, the deformation and damage processes could occur non-uniformly throughout the material.

The macroscopic aspects of creep deformation and damage are fairly well understood as a result of extensive work carried out on various materials. However, experimental investigations on the microscopic aspects such as strain distribution within individual grains, and sliding of individual grain boundaries in a polycrystalline material are far fewer. Grain boundary sliding has generally been studied by making scratch lines or optical grid lines on bicrystal specimens, and by measuring their displacement after creep testing [5–7]. In order to study the microcreep deformation behaviour of individual grains and sliding of individual grain boundaries, a novel and sensitive experimental technique using electron beam lithography has been employed [8, 9]. It consists of developing a very fine grid of electron-sensitive lines on the surface of a creep specimen and formation of electron Moiré fringes in a scanning electron microscope (SEM). The method allows simultaneous observation of the surface of the specimen and formation of Moiré fringes with features that are characteristic of the local strain distribution. In addition, these quantities can be determined by measuring the change in the spacing and offset of microgrids due to deformation and sliding. This paper describes details of the technique and its application to study microcreep deformation and grain boundary sliding behaviour of copper.

1.1. Principle of electron Moiré method

In the newly developed electron Moiré method, a scanning electron microscope equipped with a beam blanking device and a pattern generator for beam control, were employed to produce the master grid using the primary electron beam. The principle of the electron Moiré method is illustrated in Fig. 1. A scanning electron beam with spacing a_e (spacing is decided by the SEM magnification and interval of beam blanking) is exposed on the specimen surface which carries equally spaced grid lines with spacing a_m as shown in Fig. 1a. This produces electron Moiré fringes of dark and bright lines because of the difference in the amount of secondary electrons emitted from different regions of the specimen. A tensile strain in the specimen causes an increase in the spacing of the grid lines and hence produces Moiré fringes with smaller spacing (Fig. 1b). Conversely, a compressive strain leads to a decrease in the spacing of grid lines and so produces fringes with larger spacing. From the spacing of the Moiré fringes, the tensile strain ε was calculated using the following equation [10].

$$\varepsilon = [a_e/(d' - a_e)] - [(a_m - a_e)/a_e] \quad (1)$$

0022–2461

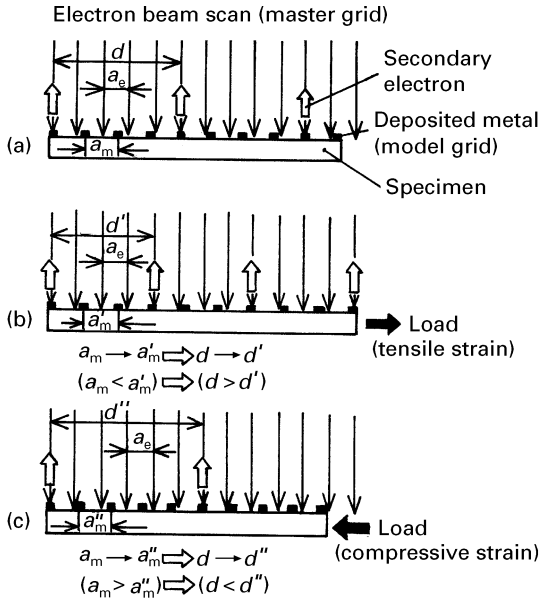

Figure 1 Schematic illustration of the principle of formation of electron beam Moiré fringes.

where d' is the distance between neighbouring Moiré fringes.

2. Experimental details

2.1. Development of microgrid

The experimental process for preparing the microgrid on the creep specimen is shown schematically in Fig. 2. A square area of about 1 mm^2 is selected on the polished specimen for the deposition of orthogonal grid lines. The selected area is spin coated with an electron-sensitive polymer film. The coated surface is exposed to the primary electron beam in an SEM with a controlled beam blanking device. The exposed resist is developed and subsequently coated with a layer of an alloy of palladium and gold which ensures good visibility in the SEM. After deposition, the remaining resist is removed by dissolving in acetone and the microgrid is now ready. The lines of the microgrid thus prepared for this investigation had a width of 1 μm, and spacing of 4.7 μm in the x and y directions. On some specimens, only parallel lines normal to the gauge length were made which had a spacing of 3.7 μm.

2.2. Creep test

Creep specimens of 3 mm thickness were machined from a 99.99% pure copper bar. The specimens were annealed at 1173 K for 30 min in argon atmosphere and subsequently quenched in water. Creep tests were carried out at 723 K at stress levels of 20 and 30 MPa in argon atmosphere. The specimen tested at 30 MPa was interrupted after 4, 15 and 21 h to carry out measurements on microdeformation and grain boundary sliding. The nominal creep strains at these test times were 1, 5 and 9%. The specimen tested at 20 MPa was interrupted after 15, 90, 140 and 165 h with corresponding creep strains of 0.3, 1.5, 2.5 and 5%.

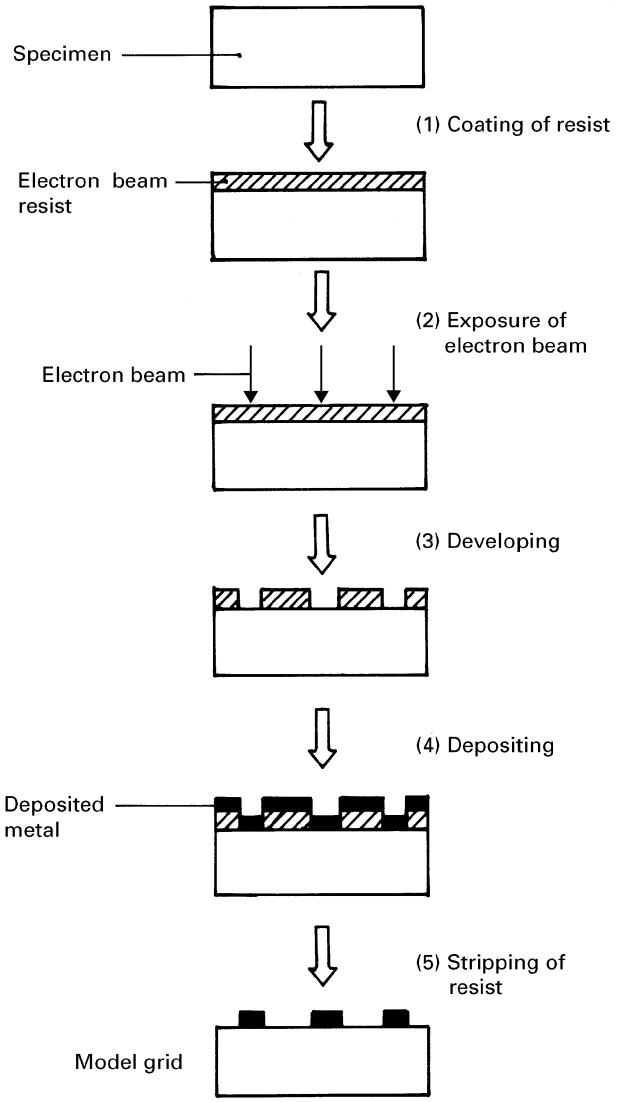

Figure 2 Flow diagram for the preparation of microgrids.

3. Results and discussion

The surface of the crept specimens showed evidence for the occurrence of several matrix and grain boundary deformation processes when examined using SEM. Fig. 3a shows microcracking at a grain boundary triple point C in the specimen tested at 20 MPa and interrupted after 90 h. A macroscopically coarse slip band BC runs through grain E, between the two grain boundary triple points B and C. Fig. 3a suggests that sliding on grain boundary AB led to stress concentration at the triple point B which induced extensive slip in grain E. The impingement of the slip band on grain boundary CD led to stress concentration on this boundary causing the nucleation of a crack which grew under the action of tensile stress. Fig. 3b is a SEM micrograph of the same region taken after 165 h of creep test. It shows coarsening of the slip band and growth of the crack as the test time increased. Although triple point cracking was the predominant mode of creep damage observed under the test conditions investigated, cavities were also seen on isolated grain boundaries.

Apart from grain boundary sliding, extensive grain boundary migration has also been observed. Fig. 4

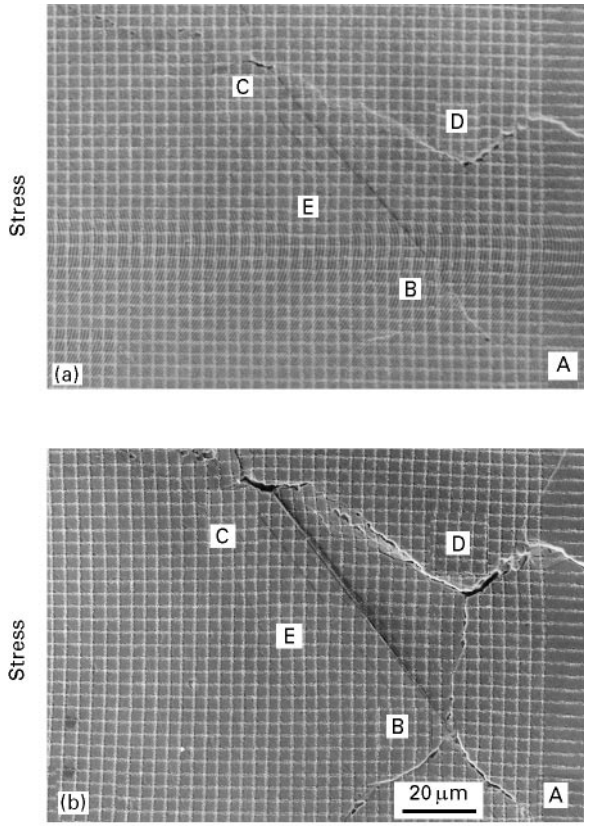

Figure 3 (a) Sliding induced slip deformation nucleating grain boundary cracks; stress, 20 MPa, time, 90 h and (b) coarsening of slip band and growth of cracks; time, 165 h.

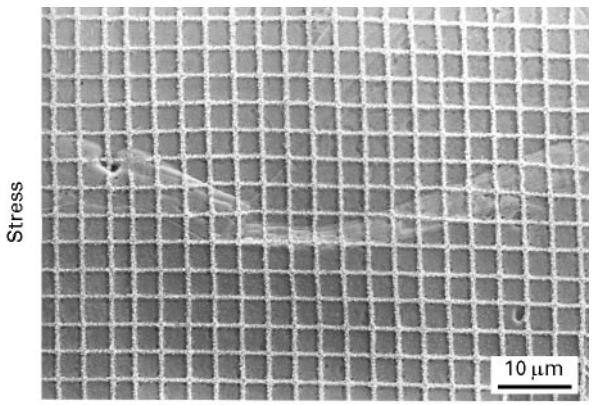

Figure 4 Migration on a grain boundary normal to the stress; stress, 20 MPa, time, 165 h.

shows a migrated boundary oriented nearly normal to the tensile stress. The migrated boundary is free from microcracks. It is considered that grain boundary migration is a healing process as it leads to postponement of damage formation or leaves the damage behind within the matrix in the case of early development of damage [2].

3.1. Microcreep deformation

In this section, the application of electron Moiré fringe and microgrid techniques for studying microdeformation of the grains is presented. Fig. 5a, b and c show electron Moiré fringes taken on a creep specimen tested at 30 MPa for 4, 15 and 21 h, respectively.

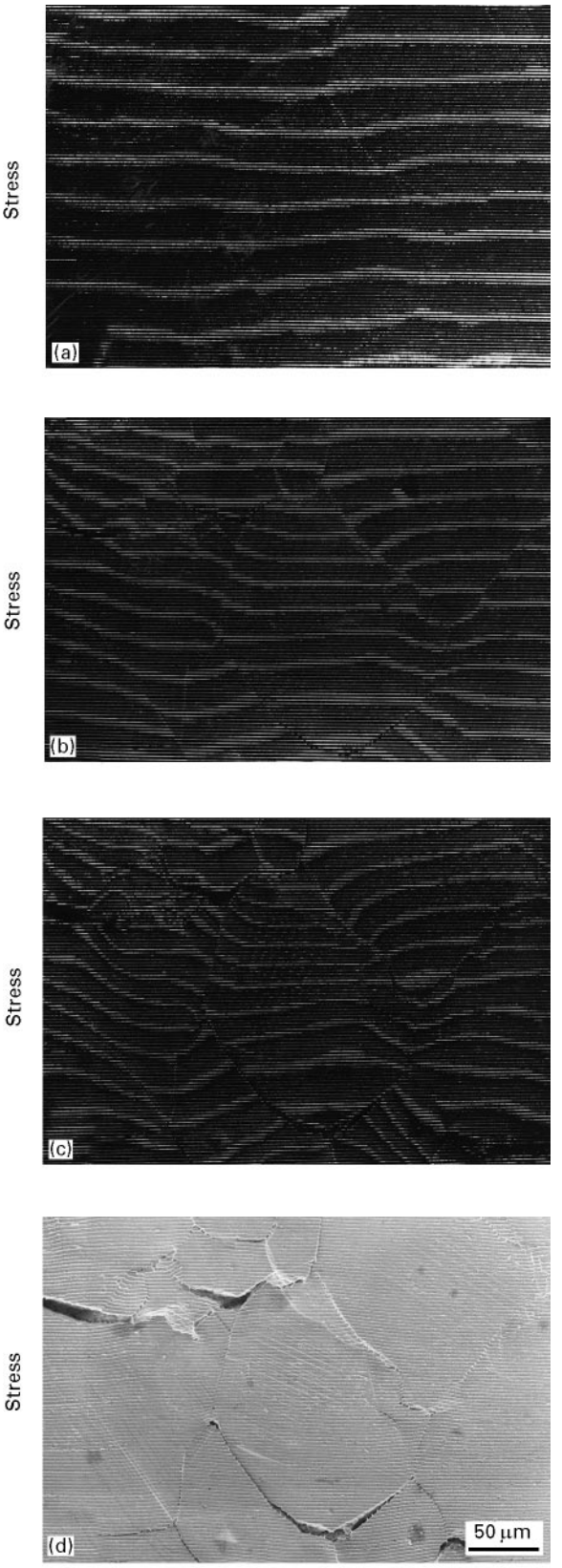

Figure 5 Moiré fringe patterns after testing at 30 MPa; time, (a) 4 h, (b) 15 h and (c) 21 h, (d) scanning electron micrograph of the same region; time, 21 h.

These fringes were formed with a scanning electron beam with a spacing of 3.5 μm. The scanning electron micrograph of corresponding to Fig. 5c is shown in Fig. 5d. One of the greatest advantages of the Moiré

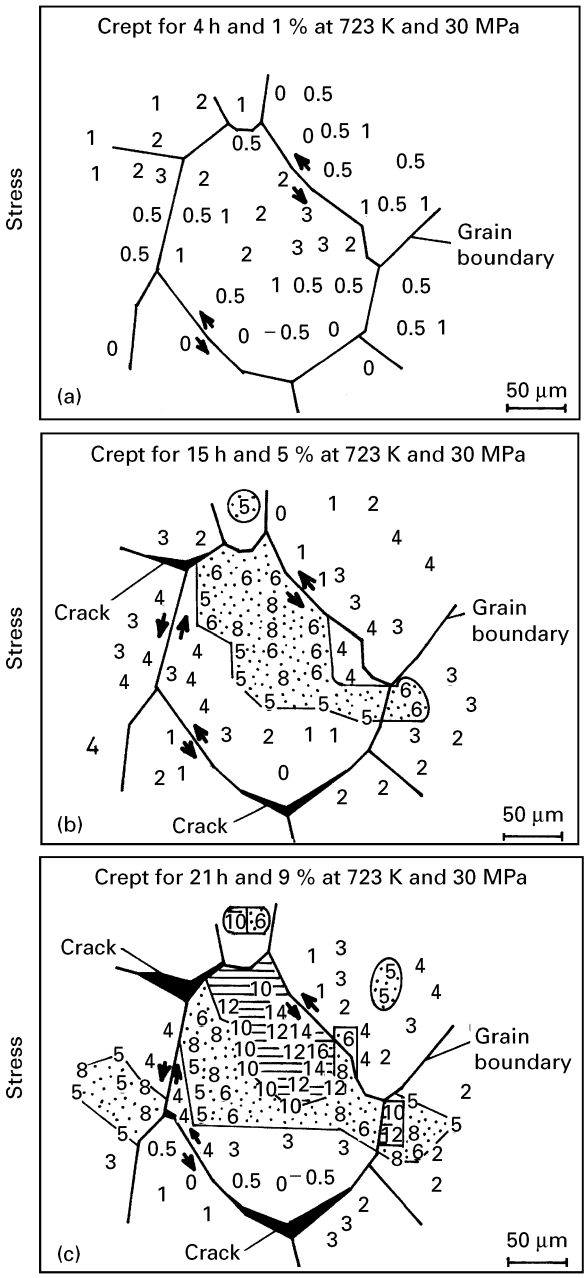

Figure 6 Microcreep strain distribution inside the grain and around the grain boundary at 30 MPa determined using Moiré fringes; (a) 4 h, (b) 15 h and (c) 21 h. Key: ▤ high tensile strain area (> 10%); ▦ medium tensile strain area (5–10%); □ low tensile strain area (< 5%); ↑ direction of grain boundary sliding. Numbers on figures represent strain, ε (%) on the spot.

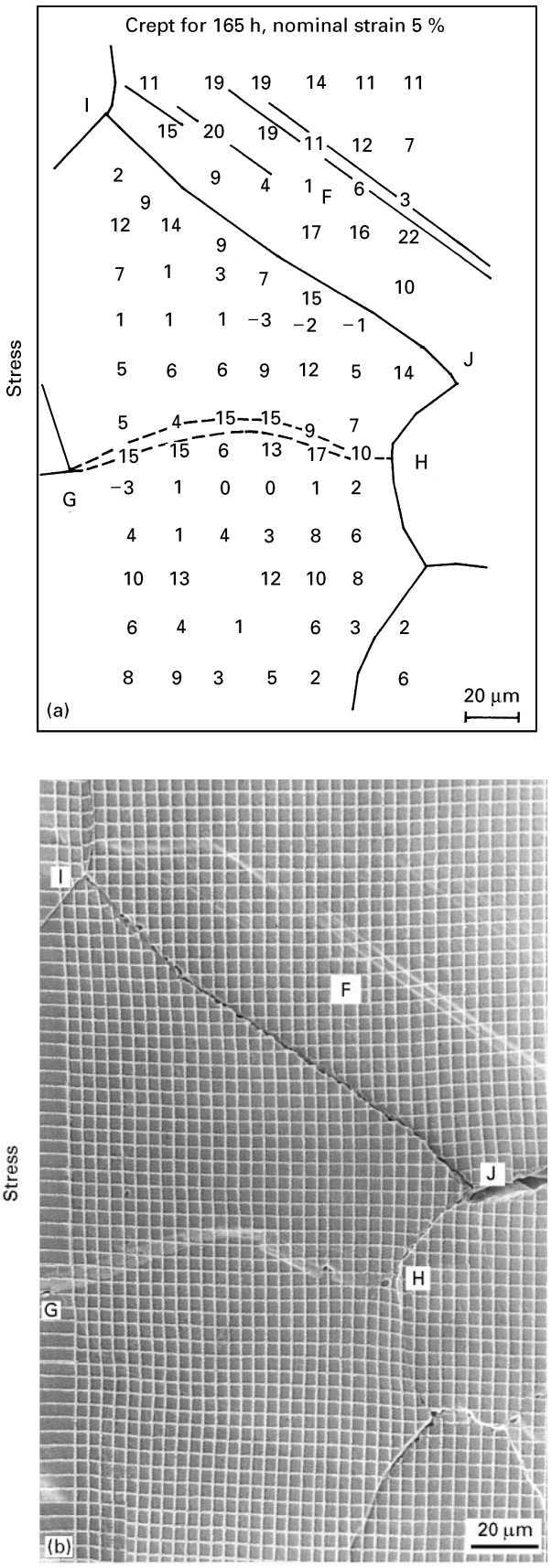

Figure 7 (a) Microcreep strain distribution inside the grain and around the grain boundary at 20 MPa determined from spacing between microgrids and (b) scanning electron micrograph of the same region. Numbers in (a) represent strain (%) on the spot.

fringe method is that it allows simultaneous observation of the specimen area from which the fringes are generated. The Moiré fringe pattern becomes complicated and the spacing of the fringes decreases as the deformation increases. Spacing of the fringes was measured in the direction parallel to the stress axis and the tensile strain was calculated using Equation 1. The distribution of microcreep strain within and around the central grain in Fig. 5a, b and c is shown in Fig. 6a, b and c for test times of 4, 15 and 21 h, respectively. In the early stages of creep, the strain distribution is nearly uniform (Fig. 6a). As creep proceeds, isolated regions of strain concentration begin to develop. The strain distribution within the central grain in Fig. 6c can be divided into three areas, namely, low strain (< 5%), medium strain (5–10%) and high strain (> 10%). The area of high strain is associated with the section of the grain boundary which exhibits high sliding. The triple point crack is

surrounded by a region of low matrix strain. This means that strain concentration due to sliding is relaxed by cracking of the boundary. Qualitatively similar results have been obtained from interrupted tests conducted at a stress level of 20 MPa.

Although the Moiré fringe technique is a very convenient and useful technique for studying strain distribution, one of the limitations of the technique is that it is capable of measuring the average strain accurately only over a length of about 50 μm or more. In order to analyse the distribution of strain over shorter distances, the change in the spacing of the microgrid lines in the direction of stress was measured using a high precision travelling optical microscope and the creep strain was determined. Fig. 7a shows the distribution of microcreep strain in the specimen tested at 20 MPa for 165 h. The corresponding SEM micrograph is shown in Fig. 7b. The following features may be noted

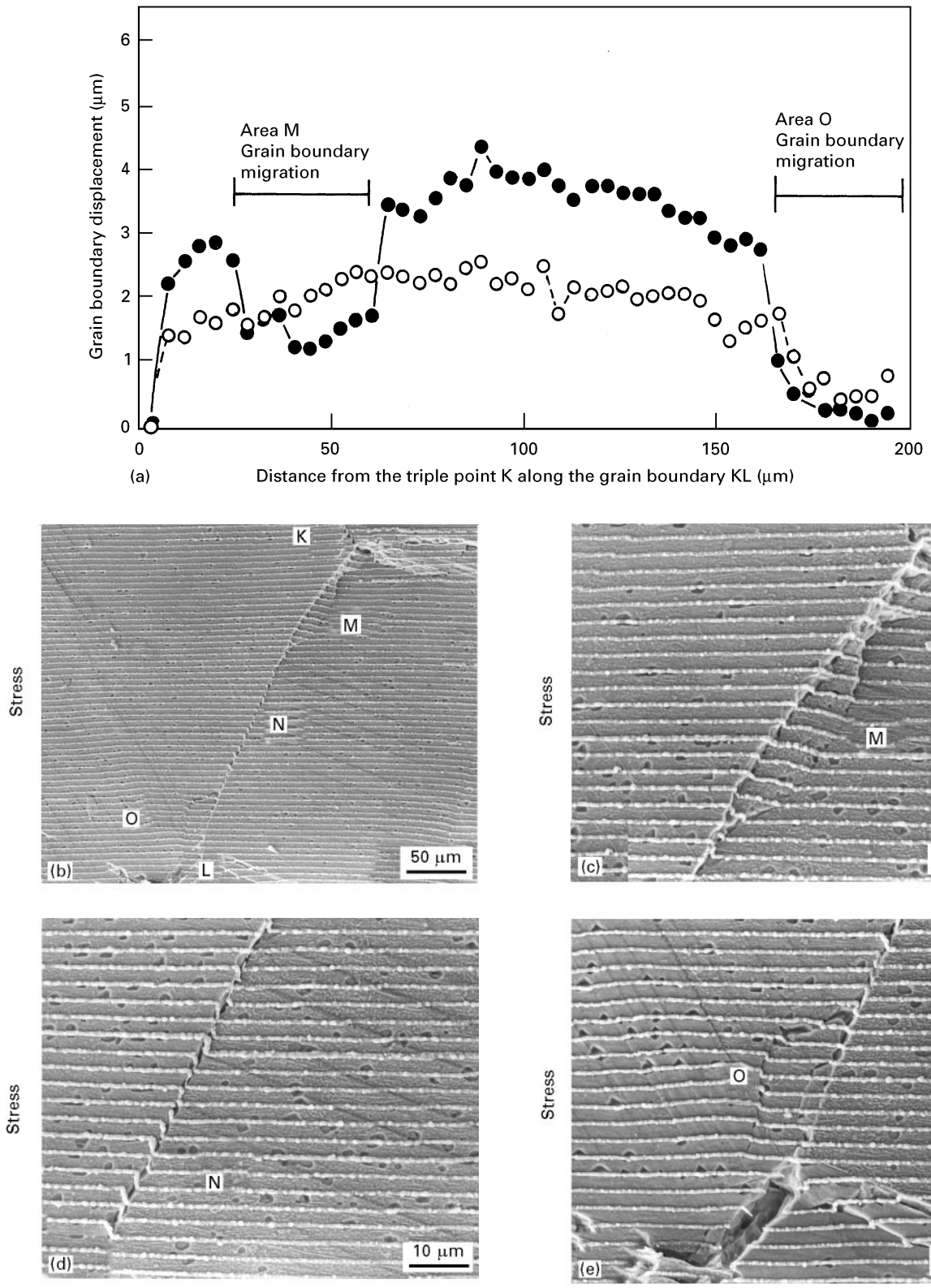

Figure 8 (a) Variation of grain boundary sliding at 30 MPa and 723 K determined from offsets of microgrids; (b), (c), (d) and (e) scanning electron micrograph of the corresponding region.

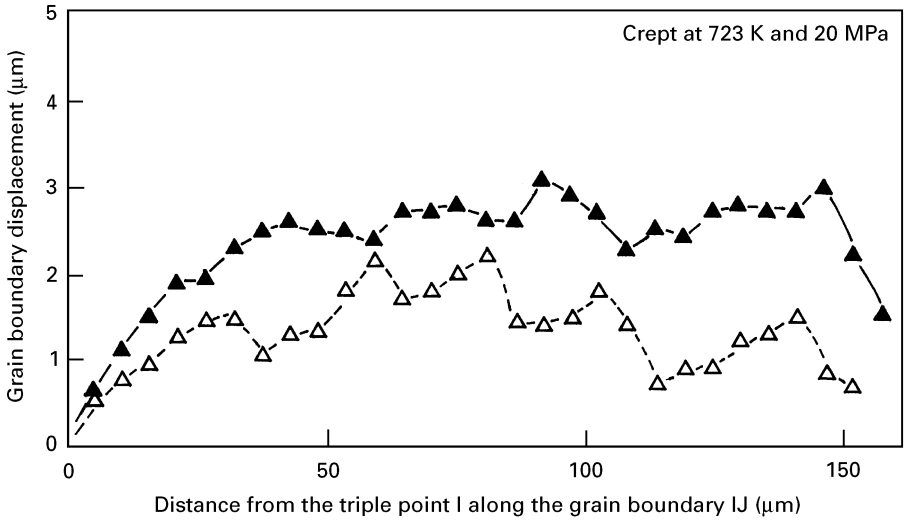

Figure 9 Variation of grain boundary sliding at 20 MPa determined from offsets of microgrids: –△– 140 h; —▲— 165 h.

from Fig. 7b: (i) coarse slip bands in the grain marked F, (ii) a migrated grain boundary marked GH and (iii) a cracked grain boundary marked IJ. Whereas the nominal creep strain at 165 h was 5%, the local strain varied very widely and in a complex manner. It is interesting to note that very high strains in the range of 10–15% exist over small regions. From Fig. 7b, it can be seen that these regions are associated with grain boundary migration or deformation bands. A small region with negative tensile strain is also observed. This is not surprising considering the fact that an earlier analysis on creep strain distribution using a multi-grained finite element model had predicted the occurrence of compressive creep strain even under tensile loading [11]. This is a consequence of non-uniform deformation taking place in adjacent grains and even in different regions of the same grain.

3.2. Grain boundary strain

Offsets in the Moiré fringes were observed across grain boundaries which have undergone sliding. The grain boundary sliding was calculated from the measured offsets and the results have been reported earlier [9]. The grain boundary displacement was determined also in terms of the offset of the microgrid lines across the grain boundary. Fig. 8a shows the variations of boundary displacement along the length of a grain boundary KL shown in Fig. 8b after 15 and 21 h of creep. The boundary displacement exhibits wavy behaviour over most of the length of the boundary and decreases drastically on approaching the triple points. This suggests that grain boundary displacement is not uniform even in a very pure metal which is devoid of any precipitate in the boundary. Instead, sliding appears to be a heterogeneous process. The factors influencing the wavy behaviour of grain boundary sliding are not clearly understood. Heterogeneity in matrix deformation, differences in the density of grain boundary ledges, and grain boundary structure may be some of the factors responsible for the observed sliding behaviour. It may be mentioned that studies of bicrystals of aluminium on the variation of boundary displacement with creep time has been reported to show a "step" behaviour [1]. It is interesting to note that the curve for 21 h dips below the curve for 15 h over two sections along the boundary. A closer examination of the grain boundary KL after 21 h of creep revealed that grain boundary migration has taken place over these sections as shown around M and O in Fig. 8c and e, respectively. There is no visible boundary migration until 15 h of deformation. The mid-section of the boundary which showed large displacement was associated with several slip bands (shown around N in Fig. 8d). It is suggested that the shear stress that causes sliding is relaxed locally when the process of migration occurs concurrently.

In cases where grain boundary sliding was not associated with migration, but has instead led to cracking (grain boundary IJ in Fig. 7b), a progressive increase in displacement with time was observed and the variation is shown in Fig. 9.

4. Conclusion

Grain boundary displacement and intragranular deformation take place non-uniformly during creep. Creep deformation exhibited localized areas of high strain associated with slip or grain boundary migration. Local strain is very low near cracked grain boundaries. Variation of grain boundary displacement along the length of the boundary showed a wavy behaviour. Boundary displacement decreases drastically when boundary migration occurs simultaneously.

Acknowledgement

One of the authors (MDM) is grateful to the Science and Technology Agency of Japan for the grant of a Fellowship under which the above research work was carried out at NRIM.

References

1. F. N. RHINES, in Proceedings of the Symposium on Creep and Fracture of Metals at High Temperatures, London, May 1954, National Physical Laboratory (Her Majesty's Stationery Office, London, 1956) p. 47.
2. T. WATANABE, *Met. Trans. A* **14** (1983) 531.
3. M. OBATA and H. SHIMADA, *J. Jpn. Inst. Met.* **40** (1976) 112.
4. J. DORN and S. MAJUMDAR, *Acta Metall. Mater.* **34** (1986) 961.
5. C. A. P. HORTON, *Acta Met. Mater.* **18** (1970) 1159.
6. R. C. GIFKINS, *Met. Trans. A* **8** (1977) 1507.
7. S. KISHIMOTO, N. SHINYA and H. TANAKA, *J. Soc. Mater. Sci. Jpn.* **37** (1988) 289.
8. S. KISHIMOTO, M. EGASHIRA, N. SHINYA and R. A. CAROLAN, in Proceedings of the Sixth International Conference on Mechanical Behaviour of Materials, Kyoto, April 1991, edited by Masahiro Jono and Tatsuo Inoue (Pergamon Press, Tokyo, 1991) p. 661.
9. S. KISHIMOTO, E. EGASHIRA and N. SHINYA, in Proceedings of Fitness-for-Service and Decision for Petroleum and Chemical Equipment, Honolulu, July 1995, edited by Erager (ASME, New York, 1992) p. 533.
10. A. VINCKIER and R. DECHAENE, *J. Basic Eng. Trans. ASME Ser. D* **82** (1960) 426.
11. R. A. CAROLAN, M. EGASHIRA, S. KISHIMOTO and N. SHINYA, *Acta Metall.* **40** (1992) 1629.

Received 14 June
and accepted 19 November 1996